Chapter 4
A Comparison of Uncertainty Quantification Methods for Damping Ratio Estimates from Tall, Modular Buildings

Patrick Brewick and John Hickey

Abstract The accurate quantification of energy dissipation is essential if the light damping ratios of tall, slender structures are to be properly leveraged during design and deployment. For instance, residential buildings, including modular construction, must adhere to rather stringent vibration criteria, often severely limiting acceptable acceleration responses. Most conventional tall buildings achieve these criteria by controlling aerodynamic loading via changes in shape over the building height, or through the addition of extra lateral stiffness via outrigger elements. However, both of these approaches are challenging to implement in modular construction. Thus, modular construction for residential projects are subject to strict vibration criteria, but lack the traditional means for vibration control. Further complicating matters, damping ratios are notoriously difficult to estimate with precision, yet design decisions are often based on the assumed or identified damping value.

This study presents a comprehensive comparison of uncertainty quantification methods for damping ratio estimation. Using acceleration data recorded in a tall, modular building, damping ratios are identified using an analytical modal decomposition within the random decrement technique. However, in order to quantify the uncertainty associated with the identified damping ratios, both bootstrapping techniques as well as a hierarchical Bayesian approach are applied. Comparative results, including statistics and confidence intervals, are provided for the first few fundamental modes along with a discussion of the capabilities of both methods.

Keywords Damping · Random decrement · Hierarchical bayesian · Bootstrapping · Analytical modal decomposition

Introduction

The response of tall buildings to environmental loads is controlled by modal properties such as the natural frequencies, mode shapes and damping ratios [1, 2]. Natural frequencies and mode shapes can be generally estimated with relative confidence; however, modal damping ratios are significantly more challenging to predict with certainty since they cannot be calculated analytically [3]. However, given their central role in structural dynamic behavior, accurate estimates of damping are crucial for predicting structural responses to dynamic loads. As a result, the improved precision of damping estimation has become an important objective within the field of system identification [4], especially when data is available from full-scale, finished structures [5, 6, 7].

Operational modal analysis (OMA) is an output-only methodology for system identification that utilizes the dynamic response of a structure without any knowledge of the exciting forces [8]. A vast range of OMA techniques have been proposed in literature, including the random decrement technique [9], stochastic subspace identification (SSI) [10], frequency domain decomposition [11], various Bayesian approaches [12, 13], and a series of enhancements and combinations of these techniques (e.g. [14, 15, 16, 17, 18]). With the notable exception of Bayesian approaches, most OMA techniques were initially

Patrick Brewick
Department of Civil and Environmental Engineering & Earth Sciences, University of Notre Dame, Notre Dame, Indiana, USA
e-mail: pbrewick@nd.edu

John Hickey
Department of Civil, Structural and Environmental Engineering, Trinity College Dublin, Dublin, Ireland
e-mail: John.Hickey@tcd.ie

© The Author(s), under exclusive license to River Publishers 2026

Kristin B. Zimmerman, PhD (eds.), *Topics in Modal Analysis & Parameter Identification in Structural Dynamics, 2026, Vol. 8*,
Conference Proceedings of the Society for Experimental Mechanics Series, https://doi.org/10.13052/rp-9788743814191

developed to return deterministic values for modal parameters of interest. However, various schemes for uncertainty quantification (UQ) have been employed or developed to augment some common deterministic OMA techniques. For instance, the perturbation-based SSI method for estimating the covariance of modal parameters [19] has been further generalized and evolved by a series of others [20, 21]. Kijewski and Kareem [22] also investigated how uncertainty in damping ratios could be quantified through bootstrapping, applying bootstrap estimates to random decrement signatures.

Conventional Bayesian frameworks, and uncertainty estimation frameworks that augment deterministic OMA techniques, typically quantify the epistemic estimation uncertainties of modal parameters [23]. However they are not designed to represent the variability in a single modal parameter estimate inferred from multiple data-sets or under varying environmental conditions. This can result in under-estimation of total parameter uncertainty [24]. This limitation has motivated the adoption of hierarchical Bayesian approaches for model calibration and model updating [24, 23, 25, 26]. Hierarchical probabilistic models introduce additional flexibility that accounts for variability in the inferred parameters while maintaining many of the strengths of the traditional Bayesian approach [27, 28]. In a structural dynamics context hierarchical models allow uncertainty in the modal parameters and hyper-parameters that define the distributions of modal parameters to be considered concurrently.

This study analyzes the fusion of bootstrapping and hierarchical Bayesian methods within OMA to more thoroughly consider the uncertainty in modal damping ratio estimates. Both approaches utilize the classical random decrement modal identification technique [9] to derive the damping ratio estimates, with an analytical modal decomposition [29] employed to isolate modal responses of interest. This study uses data from an in-situ monitoring campaign undertaken to monitor the dynamic behavior of a tall modular building, *10 Degrees*, in London, UK. While typical damping ratios have been established for conventional structures through multilateral monitoring campaigns, this is not the case for modular construction; thus, determining appropriate indicative values for use in design remains a challenge. Using the data from *10 Degrees*, this study attempts to quantify the uncertainty in the identified damping ratios of the first three fundamental modes. Moreover, the approaches developed within this study incorporate data from multiple events and channels in order to find a single, unified distribution for the modal damping ratios.

Background

The random decrement technique (RDT) [9] is a time domain-based approach for damping estimation that assumes the response of a single degree-of-freedom (SDOF) system can be decomposed into homogeneous and particular responses that are dependent on the initial conditions and forcing, respectively [30]. When response measurements, such as acceleration time histories, are available for a given structure, the RDT operates on segments of these responses. The segments are created by taking time windows of a set length wherein the first point in the window satisfies a given threshold condition that typically specifies both an amplitude x_0 and slope (or velocity) $\dot{x}_0$ criteria [22]. By setting the triggering condition to an appropriate level, multiple segments can be obtained from a given acceleration time history. It can be shown that averaging over a large number of segments with identical triggering conditions leads the ensemble averages of the initial velocity and forced response components to tend to zero, leaving only the response due to the initial displacement [9, 31]. The result is that the remaining signal represents the free decay response of the SDOF system. Given the finite duration of observed acceleration time histories in practice, the random decrement signature (RDS) can be written as

$$D_{x_0}(\tau) = \frac{1}{N_{\text{segs}}} \sum_{n=1}^{N_{\text{segs}}} \left(x_n(\tau) \middle| x_n(0) = x_0 \text{ and } \dot{x}(0) = \dot{x}_0 \right) \tag{1}$$

where $D_{x_0}(\tau)$ is the RDS, $x_n(\tau)$ represents the nth discrete segment of a given time history conditionally triggered by $x_n(0) = x_0$ and $\dot{x}(0) = \dot{x}_0$, and N_{segs} is the total number of segments.

The RDT can also be applied to multi-degree of freedom (MDOF) systems if the modes are well-separated by isolating the modal responses and treating them as SDOF systems [32]. However, a beating phenomenon can be observed in the RDS for closely spaced modes, which means the RDT cannot be directly used for evaluating the damping ratio. To overcome this issue, the RDT is commonly combined with signal decomposition methods, such as analytical modal decomposition (AMD)[29]. The AMD approach separates the frequency contents of a time series exactly; hence, it has been applied in conjunction with the RDT for damping identification in a number of studies [33, 16, 34].

The time history segments of response data that satisfy the specified trigger condition can be treated as random samples, where the set of N_{segs} segments constitutes the sample population. A bootstrap sample is formed from this population by drawing N_{segs} samples with replacement, *i.e.*, the number of samples drawn is equivalent to the number of identified segments. This operation is performed N_B times to create a set of N_B replicates. The dynamic properties, *e.g.*, damping

ratios or natural frequencies, can subsequently be estimated for each replicate. The standard error se from the replicate estimates is then obtained according to [35]

$$se = \left\{ \sum_{b=1}^{N_B} \left[\hat{\theta}^*(b) - \overline{\hat{\theta}^*} \right]^2 / (N_B - 1) \right\}^{1/2} \tag{2}$$

where $\hat{\theta}^*(b)$ represents the estimate of the dynamic property of interest based on the bth bootstrap replicate sample and $\overline{\hat{\theta}^*}$ represents the bootstrap mean, which is given by

$$\overline{\hat{\theta}^*} = \sum_{b=1}^{N_B} \hat{\theta}^*(b)/N_B \,. \tag{3}$$

Note that the standard error operates similarly to a measure of the standard deviation of the estimates. It is also essential for the sample population to be representative of the typical behavior of the actual process in order for the bootstrapping approach to work properly [22].

Estimates of the damping ratio from the RDS can also be considered from a Bayesian perspective. This study modifies the hierarchical Bayesian methodology from [25] for damping estimation via sets of modal RDS. Only a brief synopsis of the hierarchical Bayesian approach is presented herein; full details can be found in [25]. Collecting the RDS for the pth mode for every data set produces $\mathcal{D}_p = \{D_{i,p},\, i = 1, 2, \ldots, N_\mathcal{D}\}$, where $i = 1, 2, \ldots, N_\mathcal{D}$ and where $N_\mathcal{D}$ is the number of data sets. It can be assumed that an exponential decay function can predict the behavior of a given modal RDS. The ensuing prediction error, *i.e.*, the discrepancy between an estimated RDS and the model-predicted decay function $\hat{f}_{i,p}(k\Delta t; \boldsymbol{\theta}_p)$, at a given sample time $k\Delta t$ can then be defined as

$$e_{i,p}(k\Delta t; \boldsymbol{\theta}_p) = D_{i,p}(k\Delta t) - \hat{f}_{i,p}(k\Delta t; \boldsymbol{\theta}_p) \tag{4}$$

where $D_{i,p}(k\Delta t)$ represents the pth modal RDS created from the ith data set and $\boldsymbol{\theta}_p$ is a vector containing the relevant model parameters for the pth mode. Uncertainty in the prediction errors, which arises from both modeling errors and measurement noise, can be described by a zero-mean multivariate Gaussian distribution with covariance matrix $\boldsymbol{\Sigma}_p$ for each mode. The variability across data sets allows the parameter vector $\boldsymbol{\theta}_{i,p}$ to correspond to $D_{i,p}$. The covariance $\boldsymbol{\Sigma}_p$ can also be further defined as $\boldsymbol{\Sigma}_p = \{\boldsymbol{\Sigma}_{i,p}, i = 1, \ldots, N_\mathcal{D}\}$.

Adopting a hierarchical approach expands the uncertainty in $\boldsymbol{\theta}_p$ by parameterizing it as a Gaussian distribution $N(\boldsymbol{\theta}_p \,|\, \boldsymbol{\mu}_{\boldsymbol{\theta}_p}, \boldsymbol{\Sigma}_{\boldsymbol{\theta}_p})$ with mean $\boldsymbol{\mu}_{\boldsymbol{\theta}_p}$ and covariance $\boldsymbol{\Sigma}_{\boldsymbol{\theta}_p}$. Using this hierarchical framework leads to two classes of parameters: one set of data-specific parameters (in $\boldsymbol{\theta}_p$) for a given mode and another set of hyper-parameters, $\boldsymbol{\mu}_{\boldsymbol{\theta}_p}$ and $\boldsymbol{\Sigma}_{\boldsymbol{\theta}_p}$, to describe the distribution of $\boldsymbol{\theta}_p$. Based on this, the outputs from $\hat{f}_{i,p}(k\Delta t; \boldsymbol{\theta}_p)$ are conditional on $\boldsymbol{\theta}_{i,p}$, while parameter vector $\boldsymbol{\theta}_{i,p}$ is conditioned on hyper-parameters $\boldsymbol{\mu}_{\boldsymbol{\theta}_p}$ and $\boldsymbol{\Sigma}_{\boldsymbol{\theta}_p}$.

Assuming the RDS generated by the different data sets are statistically independent and that $D_{i,p}$ only depends on $\boldsymbol{\theta}_{i,p}$ and $\boldsymbol{\Sigma}_{i,p}$ allows a likelihood function to be defined as

$$\mathcal{L}(\mathcal{D}_p) = \prod_{i=1}^{N_\mathcal{D}} p(D_{i,p} | \boldsymbol{\theta}_{i,p}, \boldsymbol{\Sigma}_{i,p}) \,. \tag{5}$$

Further assuming that prediction errors $e_{i,p}(k\Delta t; \boldsymbol{\theta}_{i,p})$ from Equation 4 are independently and identically distributed (i.i.d.) according to a zero-mean Gaussian distribution with variance $\left(\sigma_e^{(i,p)}\right)^2$ allows the likelihood function for a particular RDS $D_{i,p}$ to be written as

$$\mathcal{L}(D_{i,p}) = p(D_{i,p} | \boldsymbol{\theta}_{i,p}, \boldsymbol{\Sigma}_{i,p}) = \prod_{k=1}^{n_{t_i}} \left(\sqrt{2\pi}\sigma_e^{(i,p)}\right)^{-1} \exp\left[-\frac{\left(e_{i,p}(k\Delta t; \boldsymbol{\theta}_{i,p})\right)^2}{2\left(\sigma_e^{(i,p)}\right)^2} \right] . \tag{6}$$

The prior distribution for $\boldsymbol{\theta}_{i,p}$ is defined as $N(\boldsymbol{\theta}_{i,p} | \boldsymbol{\mu}_{\boldsymbol{\theta}_p}, \boldsymbol{\Sigma}_{\boldsymbol{\theta}_p})$ while the prior distribution of the hyper-parameters can be expressed as $p(\boldsymbol{\mu}_{\boldsymbol{\theta}_p}, \boldsymbol{\Sigma}_{\boldsymbol{\theta}_p})$. Additionally, the prior distribution of $\boldsymbol{\Sigma}_{i,p}$ is not dependent on the hyper-parameters, rather it is determined by the prediction error variance. Choosing a non-informative prior for the prediction error variance and then marginalizing the joint posterior over $\boldsymbol{\Sigma}_{i,p}$ leads to [25]

$$p(\{\boldsymbol{\theta}_{i,p}\}_{i=1}^{N_\mathcal{D}}, \boldsymbol{\mu}_{\boldsymbol{\theta}_p}, \boldsymbol{\Sigma}_{\boldsymbol{\theta}_p} | \mathcal{D}_p) \propto p(\boldsymbol{\mu}_{\boldsymbol{\theta}_p}, \boldsymbol{\Sigma}_{\boldsymbol{\theta}_p}) \prod_{i=1}^{N_\mathcal{D}} \left[N(\boldsymbol{\theta}_{i,p} | \boldsymbol{\mu}_{\boldsymbol{\theta}_p}, \boldsymbol{\Sigma}_{\boldsymbol{\theta}_p}) \exp(-L_1(\boldsymbol{\theta}_{i,p})) \right] \tag{7}$$

where $L_1(\boldsymbol{\theta}_{i,p})$ is the function described by

$$L_1(\boldsymbol{\theta}_{i,p}) = -\ln\left\{\left[\sum_{k=1}^{n_{t_i}} e_{i,p}(k\Delta t, \boldsymbol{\theta}_{i,p})^2\right]^{-n_{t_i}/2}\right\}. \tag{8}$$

For large data sets the expression $\exp(-L_1(\boldsymbol{\theta}_{i,p}))$ can be asymptotically approximated by a Gaussian distribution such that $\exp(-L_1(\boldsymbol{\theta}_{i,p})) \propto N(\boldsymbol{\theta}_{i,p}\,|\,\boldsymbol{\theta}^*_{i,p}, \boldsymbol{\Sigma}^*_{\boldsymbol{\theta}_{i,p}\boldsymbol{\theta}_{i,p}})$. The mean value $\boldsymbol{\theta}^*_{i,p}$ of this distribution approximation is found through minimizing $L_1(\boldsymbol{\theta}_{i,p})$ through optimization. The covariance matrix $\boldsymbol{\Sigma}^*_{\boldsymbol{\theta}_{i,p}\boldsymbol{\theta}_{i,p}}$ for the approximation is defined as the inverse of the Hessian matrix of $L_1(\boldsymbol{\theta}_{i,p})$ evaluated at $\boldsymbol{\theta}^*_{i,p}$, *i.e.*, $[\nabla\nabla^{\mathrm{T}} L_1(\boldsymbol{\theta}_{i,p})]^{-1}_{\boldsymbol{\theta}_{i,p}=\boldsymbol{\theta}^*_{i,p}}$, where $\nabla(\cdot)$ denotes the gradient operator and $^{\mathrm{T}}$ is the transpose.

Assuming that the solution $\boldsymbol{\theta}^*_{i,p}$ to Equation 8 is globally identifiable and further marginalizing over $\boldsymbol{\theta}_{i,p}$ yields a final expression for the posterior distribution of the hyper-parameters

$$p(\boldsymbol{\mu}_{\boldsymbol{\theta}_p}, \boldsymbol{\Sigma}_{\boldsymbol{\theta}_p}|\mathcal{D}_p) \propto p(\boldsymbol{\mu}_{\boldsymbol{\theta}_p}, \boldsymbol{\Sigma}_{\boldsymbol{\theta}_p}) \prod_{i=1}^{N_{\mathcal{D}}} N(\boldsymbol{\mu}_{\boldsymbol{\theta}_p}|\boldsymbol{\theta}^*_{i,p}, \boldsymbol{\Sigma}_{\boldsymbol{\theta}_p} + \boldsymbol{\Sigma}^*_{\boldsymbol{\theta}_{i,p}\boldsymbol{\theta}_{i,p}}). \tag{9}$$

The posterior distribution of the model parameters can then be found through an application of the total probability theorem and integration over the domain over the hyper-parameters such that

$$p(\boldsymbol{\theta}_p|\mathcal{D}_p) \approx \frac{1}{N_{\mathrm{s}}} \sum_{m=1}^{N_{\mathrm{s}}} N(\boldsymbol{\theta}_p|\boldsymbol{\mu}^{(m)}_{\boldsymbol{\theta}_p}, \boldsymbol{\Sigma}^{(m)}_{\boldsymbol{\theta}_p}) \tag{10}$$

where $\boldsymbol{\mu}^{(m)}_{\boldsymbol{\theta}_p}$ and $\boldsymbol{\Sigma}^{(m)}_{\boldsymbol{\theta}_p}$ are the mth out of N_{s} total samples drawn from $p(\boldsymbol{\mu}_{\boldsymbol{\theta}_p}, \boldsymbol{\Sigma}_{\boldsymbol{\theta}_p}|\mathcal{D}_p)$.

Analysis

The data used in this study comes from acceleration recordings collected during a monitoring campaign at the *10 Degrees* development in Croydon, South London [34]. The monitoring campaign collected data from two tri-axial accelerometers installed at different locations just below roof level. The accelerometers had sampling rates of 20 Hz. While the accelerometers measured both lateral and vertical directions, this study only considers the recordings from the lateral directions, *i.e.*, each accelerometer is treated as having measurements in the x and y directions. This study analyzes data from three events during that campaign, which includes 12 total raw acceleration recordings. However, after preliminary review of the raw acceleration data, only 10 acceleration data sets were deemed fit for further analysis; two acceleration data sets from the first event had been corrupted by construction noise. The selected acceleration data is also passed through a low-pass filter to remove frequency content above 1 Hz.

Previous analyses of the building suggested that the first three primary modes are located around 0.31 Hz, 0.36 Hz and 0.44 Hz [34]. Therefore, the AMD method is formulated to decompose the acceleration data into three modal responses. The RDT technique is applied to each AMD signal, creating a collection of ten RDS for each mode. While it has been shown that damping ratio estimates are independent of trigger level, the creation of the RDS is still based on the specified triggering condition. Therefore, different trigger levels are evaluated by varying the threshold according to the standard deviation of each underlying AMD signal. The triggering levels vary from one to three standard deviations for a total of three trigger levels.

For the bootstrap analysis, a total of $N_B = 500$ bootstrap replicates, each composed of N_{segs} sample segments, are created for each modal RDS at a given trigger level. Note that the number of segments N_{segs} differs between modal RDS and trigger level. The damping ratio is estimated by fitting a decaying function to each of the N_B modal RDS.

For the Bayesian analysis, this study employs bounded uniform distributions for the prior probability density functions (pdfs) such that $\boldsymbol{\mu}_{\boldsymbol{\theta}_p} \sim U(0,1)$ for both damping ratios and natural frequencies. The covariance matrix $\boldsymbol{\Sigma}_{\boldsymbol{\theta}_p}$ is assumed to be diagonal with uniform distributions for each entry described by $\sigma_{\theta_p} \sim U(0,2)$. A direct search global optimization is utilized for minimizing Equation 8 and subsequently determining parameter vector $\boldsymbol{\theta}^*_{i,p}$. Covariance matrix $\boldsymbol{\Sigma}^*_{\boldsymbol{\theta}_{i,p}\boldsymbol{\theta}_{i,p}}$ is computed using direct differentiation to find and evaluate the Hessian at $\boldsymbol{\theta}^*_{i,p}$. When needed, a transitional Markov Chain Monte Carlo (TMCMC) method [36] is used for generating samples, where N_{s} is set at $10,000$.

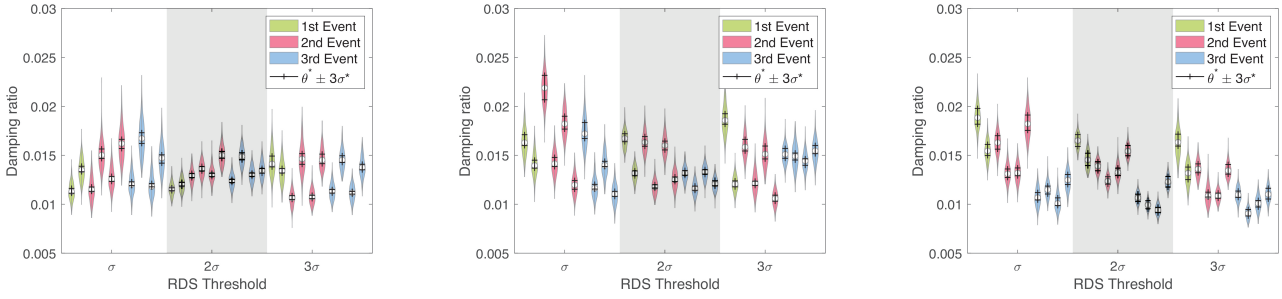
Using the estimates from the RDS with 20 periods, the asymptotic uncertainty estimates derived from the minimization of Equation 8 and its accompanying inverse Hessian are directly compared to the distributions of damping ratio estimates

derived from the bootstrapping approach for each of the first three modes in Figure 1. The mean value from the asymptotic estimates mostly coincide with the mean values from the bootstrap distributions, indicated by the white circles. There are some instances wherein the mean values are slightly different. This occurs because the damping ratio estimates are found by fitting Equation 4 for the bootstrapping approach but by minimizing Equation 8 for the asymptotic approximations within the hierarchical Bayesian method. It should also be noted that the $3\sigma^*$ bounds from the asymptotic approximations are not nearly as wide as the bootstrapping distributions. The bootstrapping results reflect estimates created from $N_B = 500$ different realizations of the modal RDS, while the asymptotic approximations are created from evaluating a single RDS. Thus, a greater degree of variation from bootstrapping is expected.

The use of $N_B = 500$ realizations also speaks to the additional computational effort required for the bootstrapping method. A benefit of the hierarchical approach is that it requires only a single evaluation of each RDS to produce uncertainty estimates. It also provides an organized framework for incorporating data from multiple events and channels. In contrast, bootstrapping requires many more RDS evaluations and does not offer a pathway for unifying uncertainty estimates outside of approaches such as ensemble averaging.

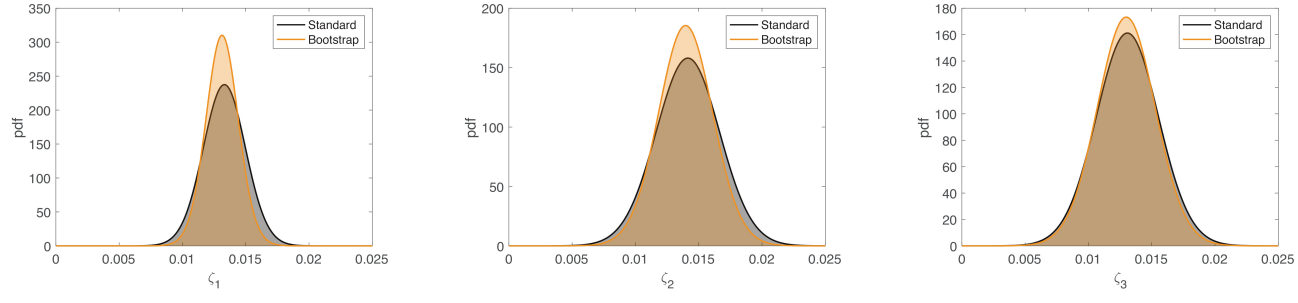
Since the bootstrap distributions are highly congruous to the uncertainty approximations made via the L_1 function in Equation 8, this study explores replacing the asymptotic approximations with the bootstrapping distributions within the hierarchical Bayesian approach. To complete this substitution, the full bootstrapping distribution cannot be directly used as the hierarchical Bayesian operates based on the mean $\boldsymbol{\theta}^*_{i,p}$ and variance $\boldsymbol{\Sigma}^*_{\boldsymbol{\theta}_{i,p}\boldsymbol{\theta}_{i,p}}$ of parameters $\boldsymbol{\theta}_{i,p}$. Thus, the mean and variance associated with each distribution is extracted for each unique combination of event, channel, and trigger threshold, just as for the original hierarchical Bayesian implementation.

Figure 2 presents a comparison of the marginal distributions for the modal damping ratios generated using both hierarchical Bayesian approaches, *i.e.*, the standard approach with individual estimates produced using L_1 and the bootstrapping substitution approach, for all three modes. The marginals generated for ζ_3 are essentially identical between cases; however, the distributions for the damping ratios of Modes 1 and 2 have some differences. For instance, the pdfs created with bootstrapping are narrower than their original counterparts. This behavior might seem unexpected considering that the boot-



(a) Mode 1 (b) Mode 2 (c) Mode 3

Fig. 1 Comparison of uncertainty in damping ratio estimates derived from bootstrapping (colored distributions) and the asymptotic approximations using Equation 8 (black lines)



(a) Mode 1 (b) Mode 2 (c) Mode 3

Fig. 2 Comparison of marginal distributions of modal damping ratios generated using the standard hierarchical Bayesian approach and bootstrapping substitution

strapping results generally return similar mean values but higher individual variances for each data set than the asymptotic approximations with Equation 8, as illustrated by Figure 1. However, the narrower distributions for the asymptotic assumptions lead to greater uncertainty in the mean value, creating a lower maximum likelihood region with a broader distribution. This effect is most pronounced for Mode 1 but can also be observed to some extent in the damping ratio distributions for Modes 2 and 3.

Conclusion

This study presents a comparative analysis of different methods for quantifying uncertainty in damping ratio estimates using data from a tall, modular building. The modular building, *10 Degrees* in London, UK, was instrumented with accelerometers whose responses are converted into RDS and subsequently utilized for damping identification via fitting of exponential decay functions. To ensure separation into modal RDS, the AMD technique is applied, which yields RDS for three fundamental modes. The uncertainty in the damping ratios is quantified through both bootstrapping and a hierarchical Bayesian approach.

The results revealed that the bootstrapping method and hierarchical Bayesian approach yield similar individual mean damping ratios while the associated variance tends to be significantly larger with bootstrapping. This was due in part to the hierarchical Bayesian method's reliance on an asymptotic assumption of uncertainty, which involved an evaluation of a single RDS, while the bootstrapping variance came from evaluations of 500 different RDS.

This study also analyzed the impact of replacing the asymptotic approximations for the individual RDS with bootstrapping statistics and found that the final distributions did not significantly change. The main notable difference was that the similar means with wider variance values from the bootstrapping results led to a more concentrated likelihood around the overall mean value and, thus, a slightly narrower distribution than that produced using asymptotic assumptions. However, the overall effect is still a similar distribution of uncertainty for a given damping ratio.

Acknowledgments The authors wish to express their thanks to the Naughton Fellowships Faculty Research Accelerator Program, which funded this research. The authors also wish to thank Tide Construction, who facilitated data gathering and supplied information about the *10 Degrees* project, as well as Shane Linehan and Vincent Barrett at Barrett Mahony Consulting Engineers for their support with this work.

References

1. Kijewski-Correa, T. and Pirnia, J.D. "Dynamic behavior of tall buildings under wind: insights from full-scale monitoring". *The structural design of tall and special buildings*, 16(4):471–486 (2007)ifnextchar.gobble.
2. Bajrić, A., Høgsberg, J., and Rüdinger, F. "Evaluation of damping estimates by automated operational modal analysis for offshore wind turbine tower vibrations". *Renewable Energy*, 116:153–163 (2018)ifnextchar.gobble.
3. Spence, S.M. and Kareem, A. "Tall buildings and damping: a concept-based data-driven model". *Journal of Structural Engineering*, 140(5):04014005 (2014)ifnextchar.gobble.
4. Brewick, P. and Smyth, A. "An investigation of the effects of traffic induced local dynamics on global damping estimates using operational modal analysis". *Mechanical Systems and Signal Processing*, 41(1-2):433–453 (2013)ifnextchar.gobble.
5. Smith, R., Merello, R., and Willford, M. "Intrinsic and supplementary damping in tall buildings". *Proceedings of the Institution of Civil Engineers - Structures and Buildings*, 163(2):111–118 (2010)ifnextchar.gobble.
6. Li, Q., Zhou, K., and Li, X. "Damping estimation of high-rise buildings considering structural modal directions". *Earthquake Engineering and Structural Dynamics*, 49(6):543–566 (2020)ifnextchar.gobble.
7. Kareem, A. and Gurley, K. "Damping in structures: its evaluation and treatment of uncertainty". *Journal of wind engineering and industrial aerodynamics*, 59(2-3):131–157 (1996)ifnextchar.gobble.
8. Rainieri, C. and Fabbrocino, G. "Operational modal analysis: overview and applications". *Strategies for reduction of the seismic risk*, pages 29–44 (2008)ifnextchar.gobble.
9. Cole, H. "On-line failure detection and damping measurement of aerospace structures by random decrement signatures". Technical Report CR-2205, NASA (1973)ifnextchar.gobble.
10. Peeters, B. and De Roeck, G. "Reference-based stochastic subspace identification for output-only modal analysis". *Mechanical systems and signal processing*, 13(6):855–878 (1999)ifnextchar.gobble.
11. Brincker, R., Zhang, L., and Andersen, P. "Modal identification of output-only systems using frequency domaindecomposition". *Smart materials and structures*, 10(3):441 (2001)ifnextchar.gobble.
12. Yuen, K.V. and Katafygiotis, L.S. "Bayesian fast Fourier transform approach for modal updating using ambient data". *Advances in Structural Engineering*, 6(2):81–95 (2003)ifnextchar.gobble.
13. Au, S.K., Zhang, F.L., and Ni, Y.C. "Bayesian operational modal analysis: theory, computation, practice". *Computers & Structures*, 126:3–14 (2013)ifnextchar.gobble.

14. Brincker, R., Ventura, C.E., and Andersen, P. "Damping estimation by frequency domain decomposition". In *Proceedings of IMAC 19: A conference on structural dynamics: Februar 5-8, 2001, Hyatt Orlando, Kissimmee, Florida, 2001*, pages 698–703. Society for Experimental Mechanics (2001)ifnextchar.gobble.
15. Hong, A.L., Ubertini, F., and Betti, R. "New stochastic subspace approach for system identification and its application to long-span bridges". *Journal of Engineering Mechanics*, 139(6):724–736 (2013)ifnextchar.gobble.
16. Wen, Q., Hua, X., Chen, Z., Niu, H., and Wang, X. "AMD-based random decrement technique for modal identification of structures with close modes". *Journal of Aerospace Engineering*, 31(5):04018057 (2018)ifnextchar.gobble.
17. Xiong, C., Wang, M., and Chen, W. "Data-driven structural dynamic characteristics investigation by combining RDT and IVMD method". *Structures*, 55:2295–2306 (2023)ifnextchar.gobble.
18. Ni, P., Yin, Z., Han, Q., and Du, X. "Output-only structural identification with random decrement technique". *Structures*, 51:55–66 (2023)ifnextchar.gobble.
19. Reynders, E., Pintelon, R., and De Roeck, G. "Uncertainty bounds on modal parameters obtained from stochastic subspace identification". *Mechanical systems and signal processing*, 22(4):948–969 (2008)ifnextchar.gobble.
20. Döhler, M. and Mevel, L. "Efficient multi-order uncertainty computation for stochastic subspace identification". *Mechanical Systems and Signal Processing*, 38(2):346–366 (2013)ifnextchar.gobble.
21. Mellinger, P., Döhler, M., and Mevel, L. "Variance estimation of modal parameters from output-only and input/output subspace-based system identification". *Journal of Sound and Vibration*, 379:1–27 (2016)ifnextchar.gobble.
22. Kijewski, T. and Kareem, A. "On the reliability of a class of system identification techniques: insights from bootstrap theory". *Structural Safety*, 24(2):261–280 (2002)ifnextchar.gobble.
23. Behmanesh, I. and Moaveni, B. "Accounting for environmental variability, modeling errors, and parameter estimation uncertainties in structural identification". *Journal of Sound and Vibration*, 374:92–110 (2016)ifnextchar.gobble.
24. Behmanesh, I., Moaveni, B., Lombaert, G., and Papadimitriou, C. "Hierarchical Bayesian model updating for structural identification". *Mechanical Systems and Signal Processing*, 64-65:360–376 (2015)ifnextchar.gobble.
25. Sedehi, O., Papadimitriou, C., and Katafygiotis, L.S. "Probabilistic hierarchical Bayesian framework for time-domain model updating and robust predictions". *Mechanical Systems and Signal Processing*, 123:648–673 (2019)ifnextchar.gobble.
26. Jia, X., Sedehi, O., Papadimitriou, C., Katafygiotis, L.S., and Moaveni, B. "Hierarchical Bayesian modeling framework for model updating and robust predictions in structural dynamics using modal features". *Mechanical Systems and Signal Processing*, 170:108784 (2022)ifnextchar.gobble.
27. Nagel, J.B. and Sudret, B. "A unified framework for multilevel uncertainty quantification in Bayesian inverse problems". *Probabilistic Engineering Mechanics*, 43:68–84 (2016)ifnextchar.gobble.
28. Brewick, P.T. "Hierarchical Bayesian calibration of deck deflection models using distributed fiber optic strain data". *Engineering Structures*, 298:117077 (2024)ifnextchar.gobble.
29. Chen, G. and Wang, Z. "A signal decomposition theorem with hilbert transform and its application to narrowband time series with closely spaced frequency components". *Mechanical systems and signal processing*, 28:258–279 (2012)ifnextchar.gobble.
30. Chopra, A.K. *Dynamics of Structures: Theory and Applications to Earthquake Engineering*. Pearson, Hoboken, NJ, 6th edition (2023)ifnextchar.gobble.
31. Vandiver, J.K., Dunwoody, A.B., Campbell, R.B., and Cook, M.F. "A mathematical basis for the random decrement vibration signature analysis technique". *Journal of Mechanical Design*, 104(2):307–313 (1982)ifnextchar.gobble.
32. Tamura, Y. and Suganuma, S.y. "Evaluation of amplitude-dependent damping and natural frequency of buildings during strong winds". *Journal of Wind Engineering and Industrial Aerodynamics*, 59(2):115–130 (1996)ifnextchar.gobble.
33. Wang, Z. and Chen, G. "Analytical mode decomposition with Hilbert transform for modal parameter identification of buildings under ambient vibration". *Engineering Structures*, 59:173–184 (2014)ifnextchar.gobble.
34. Hickey, J., Moore, H., Broderick, B., and Fitzgerald, B. "Structural damping estimation from live monitoring of a tall modular building". *The Structural Design of Tall and Special Buildings*, 33(1):e2067 (2024)ifnextchar.gobble.
35. Efron, B. and Tibshirani, R. *An introduction to the bootstrap*. Chapman and Hall, New York (1993)ifnextchar.gobble.
36. Ching, J. and Chen, Y.C. "Transitional Markov chain Monte Carlo method for Bayesian model updating, model class selection, and model averaging". *Journal of Engineering Mechanics*, 133(7):816–832 (2007)ifnextchar.gobble.